# Single-Channel Properties in Endoplasmic Reticulum Membrane of Recombinant Type 3 Inositol Trisphosphate Receptor

Don-On Daniel Mak,* Sean McBride,* Viswanathan Raghuram,* Yun Yue,* Suresh K. Joseph,§ and J. Kevin Foskett*‡

From the *Department of Physiology and ‡Institute for Human Gene Therapy, University of Pennsylvania, Philadelphia, Pennsylvania 19104; and §Department of Pathology, Thomas Jefferson University School of Medicine, Philadelphia, Pennsylvania 19107

abstract The inositol 1,4,5-trisphosphate receptor ($InsP_3R$) is an intracellular $Ca^{2+}$-release channel localized in endoplasmic reticulum (ER) with a central role in complex $Ca^{2+}$ signaling in most cell types. A family of $InsP_3Rs$ encoded by several genes has been identified with different primary sequences, subcellular locations, variable ratios of expression, and heteromultimer formation. This diversity suggests that cells require distinct $InsP_3Rs$, but the functional correlates of this diversity are largely unknown. Lacking are single-channel recordings of the recombinant type 3 receptor ($InsP_3R$-3), a widely expressed isoform also implicated in plasma membrane $Ca^{2+}$ influx and apoptosis. Here, we describe functional expression and single-channel recording of recombinant rat $InsP_3R$-3 in its native membrane environment. The approach we describe suggests a novel strategy for expression and recording of recombinant ER-localized ion channels in the ER membrane. Ion permeation and channel gating properties of the rat $InsP_3R$-3 are strikingly similar to those of *Xenopus* type 1 $InsP_3R$ in the same membrane. Using two different two-electrode voltage clamp protocols to examine calcium store-operated calcium influx, no difference in the magnitude of calcium influx was observed in oocytes injected with rat $InsP_3R$-3 cRNA compared with control oocytes. Our results suggest that if cellular expression of multiple $InsP_3R$ isoforms is a mechanism to modify the temporal and spatial features of $[Ca^{2+}]_i$ signals, then it must be achieved by isoform-specific regulation or localization of various types of $InsP_3Rs$ that have relatively similar $Ca^{2+}$ permeation properties.

key words: calcium • calcium release channel • electrophysiology • expression • *Xenopus*

## INTRODUCTION

Modulation of cytoplasmic free $Ca^{2+}$ concentration ($[Ca^{2+}]_i$) is a ubiquitous signaling system involved in the regulation of numerous cell physiological processes, in which the second messenger inositol 1,4,5-trisphosphate ($InsP_3$)[1] plays a central role in most cell types. Analysis of $InsP_3$-mediated $[Ca^{2+}]_i$ signals in single cells has revealed an unexpected complexity in numerous cell types. In the temporal domain, this complexity is manifested as repetitive spikes or oscillations, the frequencies of which are often tuned to the degree of stimulation. Observations of $[Ca^{2+}]_i$ spiking have suggested that $[Ca^{2+}]_i$ signals may be transduced not only by amplitude detection, but by frequency encoding as well (Lechleiter and Clapham, 1992; Berridge, 1993; Bootman and Berridge, 1995; Clapham, 1995; Toescu, 1995). In the spatial domain, $[Ca^{2+}]_i$ signals may initiate at specific locations in the cell and propagate as waves, at velocities ranging from 10 to 50 μm/s (Boitano et al., 1992; Amundson and Clapham, 1993; Atri et al., 1993; Rooney and Thomas, 1993). Thus, $[Ca^{2+}]_i$ signals are often organized to provide different signals to discrete parts of the cell.

$InsP_3$-mediated $[Ca^{2+}]_i$ signals are therefore precisely controlled in both time and space, resulting in a signaling system at once ubiquitous, versatile, and specific. A family of $InsP_3$ receptors ($InsP_3Rs$) with different primary sequences derived from different genes has been identified (Furuichi et al., 1989; Sudhof et al., 1991; Blondel et al., 1993; De Smedt et al., 1994; Maranto, 1994; Mignery et al., 1989) with alternatively spliced isoforms (Danoff et al., 1991; Nakagawa et al., 1991; Ferris and Snyder, 1992). The $InsP_3Rs$ are ~2,700–2,800 amino acid integral membrane proteins (Furuichi et al., 1994) that exist as tetramers (Supattapone et al., 1988; Maeda et al., 1991) in the endoplasmic reticulum (ER). The type 1 $InsP_3R$ ($InsP_3R$-1) was originally cloned from rat (Mignery et al., 1989) and mouse (Furuichi et al., 1989) cerebellum where it is expressed at high levels. Full-length $InsP_3R$-1 cDNAs have also been cloned from *Caenorhabditis elegans* (Dal Santo et al., 1999), *Drosophila* (Yoshikawa et al., 1992), *Xenopus* (Kume et al., 1993), and human (Yamada et al., 1994). The predicted sequences are 50–70% homologous.

Address correspondence to Dr. J. Kevin Foskett, Department of Physiology, University of Pennsylvania, B400 Richards Building, Philadelphia, PA 19104. Fax: 215-573-6808; E-mail: foskett@mail.med.upenn.edu

[1]*Abbreviations used in this paper:* Ab-1, $InsP_3R$-1–specific antibody; ER, endoplasmic reticulum; $InsP_3$, inositol 1,4,5-trisphosphate; $InsP_3R$, $InsP_3$ receptor; SOC, store-operated $Ca^{2+}$; TEV, two-electrode voltage-clamp.


J. Gen. Physiol. © The Rockefeller University Press • 0022-1295/2000/03/241/15 $5.00
Volume 115 March 2000 241–255
Released online 14 February 2000
http://www.jgp.org/cgi/content/full/115/3/241

Full-length sequences of cDNAs for two distinct isoforms, type 2 ($InsP_3R$-2) and type 3 ($InsP_3R$-3), have also been determined (Sudhof et al., 1991; De Smedt et al., 1994; Maranto, 1994). The three full-length sequences are 60–80% homologous (Joseph, 1995). The different isoforms have distinct and overlapping patterns of expression in different tissues (Maranto, 1994; Fujino et al., 1995; Furuichi and Mikoshiba, 1995). Most, if not all, mammalian cells examined outside the central nervous system express more than one isoform (Bush et al., 1994; De Smedt et al., 1994; Newton et al., 1994; Sugiyama et al., 1994; Fujino et al., 1995; Joseph et al., 1995; Nucifora et al., 1996), and expression levels, both absolute and relative to other isoforms, can be modified during cell differentiation (Nakagawa et al., 1991; Kume et al., 1993) and by use-dependent degradation (Magnusson et al., 1993; Wojcikiewicz et al., 1994; Honda et al., 1995; Wojcikiewicz, 1995). In tissues that express more than one $InsP_3R$ isoform, isoform-specific antibodies immunoprecipitate others, suggesting that receptors may associate in heteroligomeric complexes (Joseph et al., 1995; Monkawa et al., 1995; Wojcikiewicz and He, 1995; Nucifora et al., 1996).

This diversity of $InsP_3R$ expression is impressive, and suggests that cells require distinct $InsP_3Rs$ to regulate specific functions. Nevertheless, the functional correlates and physiological implications of this diversity are virtually unknown. That the $InsP_3R$ is a ligand-gated ion channel was originally demonstrated by tracer $Ca^{2+}$ fluxes after reconstitution of purified cerebellar type 1 receptors into liposomes (Ferris et al., 1989). The intracellular location of the $InsP_3Rs$ has restricted studies of their single-channel properties (Bezprozvanny et al., 1991; Bezprozvanny and Ehrlich, 1995; Kaftan et al., 1997), largely necessitating the use of indirect measurements to infer their channel activities; e.g., studies involving populations of $InsP_3Rs$ using measurements of $[Ca^{2+}]$ or fluxes in intact or permeabilized cells or membrane vesicles (Taylor and Richardson, 1991; Putney and Bird, 1993; Berridge, 1995). The single-channel properties of the type 1 $InsP_3R$ have been examined by reconstitution of mammalian channels in lipid bilayer membranes (Bezprozvanny et al., 1991; Watras et al., 1991; Bezprozvanny et al., 1994; Bezprozvanny and Ehrlich, 1994) and more recently by patch clamp of the outer nuclear membrane of *Xenopus* oocytes (Stehno-Bittel et al., 1995; Mak and Foskett, 1994, 1997, 1998). The type 2 receptor was recently examined by bilayer reconstitution (Perez et al., 1997; Ramos-Franco et al., 1998b). To date, there has been only one report of putative type 3 channel activity, using bilayer reconstitution of membranes from a cell type that expressed more type 3 relative to other isoforms (Hagar et al., 1998). Notably, there have been no single-channel recordings of the recombinant type 3 receptor. The $InsP_3R$-3 is a widely expressed $InsP_3R$ isoform (De Smedt et al., 1997; Newton et al., 1994) and it has been implicated in roles in addition to $Ca^{2+}$ release, including plasma membrane $Ca^{2+}$ influx in response to depletion of intracellular $Ca^{2+}$ stores (DeLisle et al., 1996; Putney, 1997) and in apoptosis (Khan et al., 1996). Here, we describe the first functional expression and single-channel recording of recombinant rat $InsP_3R$-3 (r-$InsP_3R$-3) in its native membrane environment. The approach we describe suggests a novel general strategy for successful expression and recording of recombinant ER-localized ion channels in the ER membrane. Use of conditions that were similar to those previously employed in studies of the endogenous type 1 $InsP_3R$ channel in the outer nuclear membrane has now enabled the first comparison of the permeation and gating properties of different $InsP_3R$ isoforms in the same native membrane environment. Our results demonstrate that the ion permeation and channel gating properties of the r-$InsP_3R$-3 channel in the ER membrane are remarkably similar in most respects to those of the *Xenopus* $InsP_3R$-1 (*X*-$InsP_3R$-1) in the same membrane. The similarities of permeation and gating properties of $InsP_3Rs$ between isoforms and species suggest that if cellular expression of multiple $InsP_3R$ isoforms is a mechanism to modify the temporal and spatial features of $[Ca^{2+}]_i$ signals, then it must be achieved by isoform-specific regulation and/or localization of various types of $InsP_3Rs$ that have relatively similar channel gating and permeation properties.

## MATERIALS AND METHODS

### *Synthesis of r-$InsP_3R$-3 cRNA for Expression in Xenopus Oocytes*

Rat $InsP_3R$-3 cDNA was introduced into a modified pSP64 vector by digesting pSP-CFTR (provided by Dr. B. Skach, Oregon State University of the Health Sciences, Corvallis, OR) with Ava1 and Xba1 to remove the CFTR cDNA. The vector was blunt-ended with $T_4$ DNA polymerase, religated with $T_4$ ligase, linearized with EcoR1, and ligated by $T_4$ DNA ligase to a Not1/EcoR1 adapter sequence. The new vector was linearized by Not1 and dephosphorylated by calf intestinal alkaline phosphatase. $InsP_3R$-3 cDNA was excised from pCB6-$InsP_3R$-3 (provided by Dr. G. Bell, University of Chicago, Chicago, IL) by Not1, purified (Geneclean III kit; Bio 101, Inc.), and introduced into pSP64 to create pSP-$InsP_3R$-3. Plasmid DNA of selected clones of transfected *Escherichia coli* was digested to verify the orientation and sequence of subcloned cDNAs. The final selected clones were amplified, and plasmid DNA was extracted and purified (plasmid purification kit; QIAGEN Inc.). In vitro transcribed cRNA was synthesized using the RiboMAX Large Scale RNA Production System (Promega Corp.).

### *Selection and Microinjection of Xenopus Oocytes*

Maintenance of *Xenopus laevis* and surgical extraction of ovaries were carried out as described previously (Mak and Foskett, 1994, 1997, 1998). Because oocytes have an endogenous $InsP_3R$-1 (*X*-$InsP_3R$-1), it was necessary to distinguish them from expressed channels in our patch-clamp experiments using isolated oocyte

nuclei. Endogenous channel activity detected in patch-clamp experiments using oocyte nuclei is highly variable from batch to batch of oocytes, although the activity level among oocytes from the same batch is very consistent (Mak and Foskett, 1994). It has been common to find batches of oocytes that fail to exhibit any channel activity when their nuclei are patched. Although this has been a significant problem in our studies of the *X*-$InsP_3R$-1, we reasoned that it would enable the use of this system for expression studies by providing a null background. Therefore, for each new batch of oocytes, a day of patch clamping of isolated nuclei (at least six nuclei, 6–10 patches from each) was performed to determine the endogenous channel expression. Only batches with extremely low channel activity (<1 of 15 patches exhibited $InsP_3R$ channel activity) were used for subsequent cRNA injections.

Oocytes selected for microinjection were defolliculated (Jiang et al., 1998). *Xenopus* ovaries were mechanically separated into pieces containing five or fewer oocytes each, and treated with 2 mg/ml solution of collagenase type IV (Sigma Chemical Co.) in $Ca^{2+}$-free SOS (100 mM NaCl, 2 mM KCl, 1 mM $MgCl_2$, 5 mM HEPES, pH adjusted to 7.6 with NaOH) at room temperature for 1 h. Defolliculated oocytes were washed four to five times and kept in SOS (same as $Ca^{2+}$-free SOS except with 1.8 mM $CaCl_2$), and then used for injection <24 h after defolliculation.

23 nl of cRNA (1 μg/μl) was injected into the cytoplasm of defolliculated oocytes using a nanoliter injector (World Precision Instruments) (Goldin, 1992). cRNA-injected and uninjected but defolliculated control oocytes were placed in individual wells in 96-well plates containing 200 μl of ASOS [SOS with 3 mM Na pyruvate, 100 μg/ml gentamycin, and 100 μM ALLN (*N*-acetyl-Leu-Leu-Norleucinal; Sigma Chemical Co.)]. 80 μl of ASOS in each well was changed daily. Patch clamp and two-electrode voltage clamp studies using injected oocytes were performed 4–5 d after cRNA microinjection.

### *Western Analysis*

For each sample, 10 oocytes were placed in 200 μl of ice-cold oocyte extraction buffer [OEB, containing 150 mM NaCl, 100 mM TrisHCl, 10 mM EDTA, 1% Triton X100 (wt/vol), pH 8.0] with protease inhibitor mix (1 mM PMSF, 1 μM pepstatin A,1 μM leupeptin, 10 μM E-64; Sigma Chemical Co.) and homogenized. The homogenate was placed on ice for 30 min, and then spun at top speed for 15 min on a bench-top centrifuge (Eppendorf). 150 μl of the clear supernatant, excluding the top emulsion layer from yolk, was extracted. 15 μl of the clear extract (approximately equivalent to one oocyte) was separated by 5% SDS-PAGE, transferred to nitrocellulose, and analyzed by blotting with an $InsP_3R$-1–specific antibody (Ab-1; Joseph and Samanta, 1993; Joseph et al., 1995), or an $InsP_3R$-3–specific antibody (Ab-3; Transduction Laboratories) and detected by enhanced chemiluminescence (Amersham Pharmacia Biotechnology).

### *Immunoprecipitation*

The protocol used was modified from that used for immunoprecipitation of $InsP_3Rs$ from WB cell extracts (Joseph et al., 1995). For each sample, 15 oocytes were placed in 300 μl of ice-cold OEB with protease inhibitor mix and homogenized. 225 μl of clear oocyte extract was obtained as described for Western analyses. The extract was precleared for 2 h with 40 μl of protein A agarose [50% slurry (vol/vol); GIBCO BRL], and then treated overnight with Ab-1. Immune complexes of Ab-1 and *X*-$InsP_3R$-1 were precipitated with protein A agarose pretreated with OEB containing 1% bovine serum albumin. The immunoprecipitated complexes were washed once using ice-cold OEB with an additional 350 mM NaCl and 1% SDS and twice using ice-cold OEB, separated by 5% SDS-PAGE, transferred to nitrocellulose, immunoblotted with Ab-3, and detected by enhanced chemiluminescence. Similar oocyte samples were precleared with protein G agarose [50% slurry (vol/vol); GIBCO BRL], treated overnight with Ab-3, immunoprecipitated with BSA-pretreated protein G agarose, washed, and immunoblotted with Ab-1.

### *Patch Clamping the Oocyte Nucleus*

Patch-clamp experiments were performed as described previously (Mak and Foskett, 1994, 1997, 1998). In brief, stage V or VI oocytes were opened mechanically just before use. The nucleus was separated from the cytoplasm and transferred to a dish on the stage of a microscope for patch clamping. Due to channel inactivation (Mak and Foskett, 1994, 1997), unless stated otherwise, experiments were done in "on-nucleus" configuration, with the solution in the perinuclear lumen between the outer and inner nuclear membranes in apparent equilibrium with the bath solution (Mak and Foskett, 1994). Following standard conventions, the applied potential is that of the pipette electrode minus the reference bath electrode (positive current flows from pipette outward). Experiments were performed at room temperature.

Single-channel currents were amplified with an Axopatch-1D amplifier (Axon Instruments) with anti-aliasing filtering at 1 kHz, transferred to a Power Macintosh 8100 via an ITC-16 interface (Instrutech Corp.), digitized at 5 kHz, and written directly onto hard disk by Pulse+PulseFit software (HEKA Elektronik). Data were analyzed and fitted with theoretical curves using MacTac 3.0 (Bruxton), and Igor Pro 3 (WaveMetrics).

### *Solutions for Patch-clamp Experiments*

Unless stated otherwise, the pipette solutions used in patch-clamp experiments contained (mM): 140 KCl, 10 HEPES, 0.5 $Na_2ATP$, pH adjusted to 7.1 with KOH with 0 or 3 $MgCl_2$. Because of chelation of $Mg^{2+}$ by ATP, the actual free $Mg^{2+}$ in the solutions was 0 or 2.5 mM. By using $K^+$ as the current carrier and appropriate quantities of the high-affinity $Ca^{2+}$ chelator, BAPTA [100–500 μM 1,2-bis(*O*-aminophenoxy) ethane-*N*,*N*,*N*′,*N*′-tetraacetic acid; Molecular Probes, Inc.], or the low-affinity $Ca^{2+}$ chelator, 5,5′-dibromo BAPTA (100–400 μM; Molecular Probes, Inc.), or just ATP (0.5 mM) to buffer [$Ca^{2+}$] in the experimental solutions, [$Ca^{2+}$] was tightly controlled in our experiments. Total $Ca^{2+}$ content in the solutions (5–350 μM) was determined by induction-coupled plasma mass spectrometry (Mayo Medical Laboratory, Rochester, MN). Free [$Ca^{2+}$] were calculated using the Maxchelator software (C. Patton, Stanford University, Stanford, CA). Pipette solutions contained various concentrations of $InsP_3$ (Molecular Probes, Inc.) as stated. Unless stated otherwise, all patch-clamp experiments used a bath solution with the same composition as the pipette solutions except with no $Na_2ATP$ or $MgCl_2$, and calculated free $Ca^{2+}$ concentration of 250 nM.

In ion selectivity determinations, the low $K^+$ solution contained 110 mM *N*-methyl-d-glucamine Cl, 30 mM KCl, 10 mM HEPES, 1.27 mM BAPTA, pH adjusted to 7.1 by KOH. [$Ca^{2+}$] was calculated to be 2 μM. The high $Ca^{2+}$ solution contained 50 mM $CaCl_2$, 45 mM *N*-methyl-d-glucamine Cl, 30 mM KCl, 10 mM HEPES, pH adjusted to 7.1 by KOH.

### *Oocyte Two-Electrode Voltage-clamp Experiments*

Conventional two-electrode voltage-clamp (TEV) methods (Stühmer, 1992) were used to measure membrane currents in either $InsP_3R$-3–expressing oocytes ($InsP_3R$ cRNA injected, with functional expression confirmed by patch clamping of isolated nuclei), or uninjected control oocytes, using an OC-725C oocyte clamp amplifier (Warner Instrument Corp.) connected to a Pow-

erMac 7100 via an ITC-16 interface. Single oocytes were placed in a chamber (0.6 ml vol) containing a low-$Ca^{2+}$ solution LCa96 (96 mM NaCl, 1 mM KCl, 0.2 mM $CaCl_2$, 5.8 mM $MgCl_2$, 10 mM HEPES, pH 7.5 by NaOH). Pulse+PulseFit software was used to ramp the applied transmembrane potential ($V_m$) at regular intervals. $V_m$ was clamped at the prestimulation reversal potential in between the voltage ramps. Transmembrane current ($I_m$) and $V_m$ were digitized at 1 kHz during the voltage ramps and written directly onto hard disk. The whole-oocyte membrane conductance was evaluated as the slope ($dI_m/dV_m$) of a fifth-order polynomial (Jiang et al., 1998) fitted to the raw, monotonically increasing $I_m - V_m$ curve from each voltage ramp using Igor Pro 3 software.

In experiments that monitored changes in $[Ca^{2+}]_i$ by measuring the plasma membrane $Ca^{2+}$-activated $Cl^-$ current ($I_{Cl\text{-}1}$ described by Hartzell, 1996), $V_m$ was ramped from −60 to 20 mV in 550 ms, repeated at 1-s intervals. The membrane conductance was evaluated at $V_m$ = 10 mV. To provide sustained stimulation to activate the $InsP_3R$ maximally, 23 nl of 10 μM $InsP_3$ was repeatedly (90-s intervals) microinjected into the voltage-clamped oocytes using a nanoliter injector (Hartzell, 1996). After relaxation of the $InsP_3$-induced membrane current to a steady level (usually 250–300 s after first injection of $InsP_3$), 6 ml of high-$Ca^{2+}$ solution HCa96 (same composition as LCa96 except with 5.8 mM $CaCl_2$ and 0.2 mM $MgCl_2$) was perfused into the oocyte chamber, and the $Cl^-$ current induced by $Ca^{2+}$ influx through the store-operated $Ca^{2+}$ channel, $I_{SOC}$ described in Hartzell (1996), was recorded.

In experiments designed to measure $I_{SOC}$ directly, protocols previously described in Yao and Tsien (1997) were followed. $Ca^{2+}$ store depletion was accomplished by extracellular application of fetal bovine serum (1:100) in LCa96 (Miledi and Parker, 1989). $V_m$ was ramped from −100 to 50 mV in 700 ms, repeated at 3-s intervals. Contributions to the membrane current by the $Ca^{2+}$-activated $Cl^-$ channels were minimized by microinjection of $Ca^{2+}$ chelator—41.4 nl of 100 mM BAPTA for a final concentration of ~4 mM (Yao and Tsien, 1997); and evaluating the conductance at $V_m$ = −80 mV, where the $Ca^{2+}$-activated $Cl^-$ channels ($I_{Cl\text{-}1}$ and $I_{Cl\text{-}2}$) were least active (Hartzell, 1996). The bathing LCa96 solution was replaced with HCa96 by perfusion of 6 ml of HCa96 into the oocyte chamber to observed $I_{SOC}$ directly.

## RESULTS

### *Expression of r-InsP$_3$R-3 in Xenopus Oocytes*

Multiple isoforms of $InsP_3R$ exist in mammalian cells, coded by different genes and expressed in distinct and overlapping patterns in various tissues. To determine whether different isoforms exhibit distinct single-channel properties, we used *Xenopus* oocytes because we have demonstrated that it is possible to record $InsP_3R$ channel activity in their isolated nuclei (Mak and Foskett, 1994, 1997, 1998), and oocytes can efficiently express mammalian ion channel proteins from injected cRNAs and cDNAs (Soreq and Seidman, 1992). Oocytes microinjected with the cRNA of r-$InsP_3R$-3 were sampled at various times after microinjection for biochemical determinations of $InsP_3R$-3 expression. Western blot analysis using a specific $InsP_3R$-3 antibody (Ab-3) revealed a band at the appropriate molecular weight (~250 kD) in cRNA-injected oocytes (Fig. 1 B) that was not present in uninjected control oocytes (A), confirming expression of r-$InsP_3R$-3 in oocytes by cRNA injection. Expression was detectable as early as 7 h after injection, and increased to a steady level by 48 h after injection. Expression level then remained constant up to 5 d after injection, before declining (not shown).

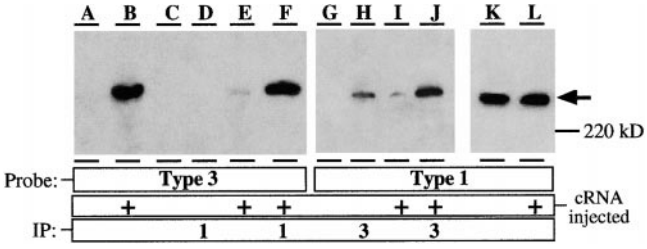


Figure 1. Expression of endogenous type 1 and recombinant type 3 $InsP_3$ receptors in *Xenopus* oocytes. (A–F) Immunoblotted with Ab-3; (G–K) immunoblotted with Ab-1. (A) Western blot of lysate from an equivalent of one control oocyte, demonstrating lack of endogenous type 3 $InsP_3R$ expression; (B) Western blot of lysate from an equivalent of one r-$InsP_3R$-3 cRNA-injected oocyte, demonstrating expression of the recombinant r-$InsP_3R$-3 protein; (C) Western blot of type 3 $InsP_3R$ adsorbed nonspecifically to agarose beads, from lysate from fifteen control oocytes; (D) Western blot of type 3 $InsP_3R$ in $InsP_3R$-1 immunoprecipitate, from lysate from fifteen control oocytes; (E) Western blot of type 3 $InsP_3R$ adsorbed nonspecifically to agarose beads, from lysate from fifteen cRNA-injected oocytes; (F) Western blot of type 3 $InsP_3R$ in $InsP_3R$-1 immunoprecipitate from lysate, from fifteen cRNA-injected oocytes. Difference between F and E represents the amount of recombinant r-$InsP_3R$-3 specifically immunoprecipitated with *X*-$InsP_3R$-1. (G) Western blot of *X*-$InsP_3R$-1 adsorbed nonspecifically to agarose beads, from lysate from fifteen control oocytes; (H) Western blot of *X*-$InsP_3R$-1 in $InsP_3R$-3 immunoprecipitate, from lysate from fifteen control oocytes. The $InsP_3R$ detected is most likely caused by cross-interaction of the immunoprecipitating Ab-3 with the large amount of endogenous *X*-$InsP_3R$-1 present in the lysate from fifteen oocytes. (I) Western blot of *X*-$InsP_3R$-1 adsorbed nonspecifically to agarose beads, from lysate from fifteen cRNA-injected oocytes; (J) Western blot *X*-$InsP_3R$-1 in $InsP_3R$-3 immunoprecipitate, from lysate from fifteen cRNA-injected oocytes. Difference in protein amounts between H/I and J represents the amount of *X*-$InsP_3R$-1 specifically immunoprecipitated with recombinant r-$InsP_3R$-3. (K) Western blot of *X*-$InsP_3R$-1 in lysate from an equivalent of one control oocyte; (L) Western blot of *X*-$InsP_3R$-1 in lysate from an equivalent of one cRNA-injected oocyte. Comparisons of K and L indicate that r-$InsP_3R$-3 expression does not induce changes in the expression levels of the endogenous *X*-$InsP_3R$-1. Western blots of type 1 $InsP_3R$ in $InsP_3R$-1 immunoprecipitates or type 3 $InsP_3R$ in $InsP_3R$-3 immunoprecipitates are not shown because too much protein was present in those lanes for the protein bands to be properly detected with the same exposure as the other lanes.

### *Functional Detection of r-InsP$_3$R-3 Expressed in Oocytes*

To reduce the likelihood of detecting endogenous *X*-$InsP_3R$-1 channels in patch-clamp experiments using r-$InsP_3R$-3 cRNA-injected oocytes, we determined the level of functional expression of the endogenous *X*-$InsP_3R$-1 channel in the outer nuclear envelope by patch-clamp experiments on isolated nuclei from freshly procured oocytes (uninjected). As described in materials and methods, batch-to-batch variability among oocytes

in the functional expression of endogenous *X*-$InsP_3R$-1 enabled suitable oocytes with sufficiently low endogenous channel activity to be chosen for expression studies of recombinant r-$InsP_3R$-3. We selected for cRNA microinjection only batches of oocytes in which the probability of detecting *X*-$InsP_3R$-1 activity in a nuclear patch-clamp experiment (with 10 μM $InsP_3$ in the pipette) was extremely low: <1 of 15 patches exhibited endogenous $InsP_3R$ channel activity. Of 336 nuclear patches from uninjected oocytes in such selected batches, only 17 channels were detected in nine patches. The mean number of $InsP_3R$ channels per nuclear patch ($\langle n \rangle$) was 0.051. The probability of detection of endogenous $InsP_3R$ in nuclear envelopes of uninjected control oocytes maintained under identical conditions as cRNA-injected oocytes never increased over time. On the other hand, the probability of detecting $InsP_3R$-like channel activities increased dramatically in injected oocytes measured 4–5 d after cRNA microinjection. In 767 experiments, 1,546 channels were detected in 381 patches, with 286 patches exhibiting multiple $InsP_3R$ channels. $\langle n \rangle$ for the cRNA-injected oocytes increased to 2.02. Thus, the r-$InsP_3R$-3 cRNA injection into appropriately selected batches of oocytes resulted in a >40-fold increase in the mean number of $InsP_3R$ channels detected by nuclear patch-clamp experiments.

The channel activities detected in the nuclei from the cRNA-injected oocytes (Fig. 2 A) were highly reminiscent of those displayed by the *X*-$InsP_3R$-1 (B) (Mak and Foskett, 1994, 1997). Two sets of experiments were conducted to confirm their identities as $InsP_3$-sensitive channels. First, in multiple nuclear patches with the pipette solutions alternately containing either 10 μM or no $InsP_3$, the channels were only detected in the presence of $InsP_3$ (59 channels in 13 patches from three nuclei), but not in its absence (zero channels in seven patches). Second, the channel activities were completely suppressed by the competitive $InsP_3$ inhibitor heparin (100 μg/ml) in all nine patches obtained from five nuclei, which showed 55 channels in 22 patches without heparin. These pharmacological results, together with the statistical data above, strongly suggested that the channel activities observed in nuclei from cRNA-injected oocytes were recombinant r-$InsP_3R$-3 expressed due to the cRNA injection.

Two additional sets of evidence further indicated that the $InsP_3R$ detected in patch-clamp experiments using nuclei from cRNA-injected oocytes were not contributed by the endogenous *X*-$InsP_3R$-1. First, a series of Western blot analyses of cRNA-injected oocytes conducted using a type 1 isoform-specific antibody (Ab-1) demonstrated that there was no detectable increase in the expression levels of the endogenous *X*-$InsP_3R$-1 in the oocytes injected with r-$InsP_3R$-3 cRNA compared with the uninjected ones (Fig. 1, K and L). Thus, the 40-fold greater

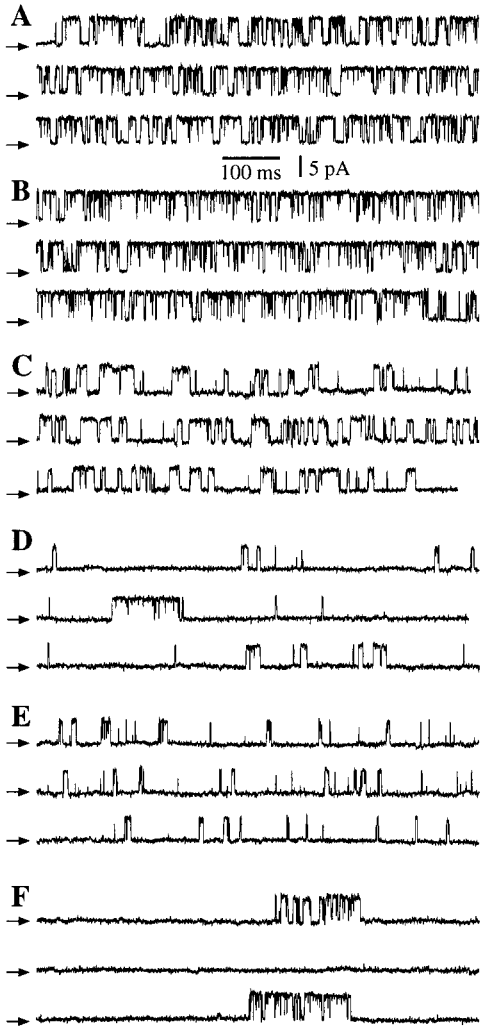


Figure 2. Current traces obtained by patch clamping the outer membrane of isolated oocyte nuclei in symmetric 0-mM $Mg^{2+}$ solutions. All current records shown were obtained with $V_{app}$ = 20 mV, and with 0.5 mM free ATP and 10 μM $InsP_3$ in the pipette solution. The arrows indicate the closed channel current level. (A, C, and E) Nuclei from r-$InsP_3R$-3 cRNA-injected oocytes. (B, D, and F) Nuclei from uninjected oocytes. (A and B) $[Ca^{2+}]_i$ = 1,150 nM. (C and D) $[Ca^{2+}]_i$ = 80 nM. (E and F) $[Ca^{2+}]_i$ = 57.5 μM. The average $P_o$ (±SEM) evaluated for *n* experiments under the shown experimental conditions are: (A) 0.75 ± 0.03 (*n* = 16); (B) 0.80 ± 0.02 (*n* = 8); (C) 0.45 ± 0.07 (*n* = 4); (D) 0.14 ± 0.03 (*n* = 7); (E) 0.23 ± 0.07 (*n* = 4); (F) 0.27 ± 0.11 (*n* = 6).

number of $InsP_3R$ channels observed in cRNA-injected oocyte nuclei was not caused by upregulation of *X*-$InsP_3R$-1 expression. Second, although the $InsP_3R$ channel activities observed in cRNA-injected oocyte nuclei when $[Ca^{2+}]_i > 1$ μM were similar to those previously observed in uninjected oocyte nuclei (Mak and Foskett, 1994, 1997, 1998) (Fig. 2, A and B), and the channel activities in both injected and uninjected oocyte nuclei exhibited dramatic inhibition by $[Ca^{2+}]_i > 50$ μM (Fig. 2, E and F), when $[Ca^{2+}]_i$ was lowered to <500 nM, $InsP_3R$

channels from r-Ins$P_3$R-3 cRNA-injected oocytes gated with a significantly higher open probability ($P_o$) than those from uninjected oocytes (Fig. 2, C and D). Thus, the channels observed upon expression of recombinant r-Ins$P_3$R-3 were distinguishable from the endogenous channels. Taken together, these results strongly suggest that the channel activities we recorded in the present work were those of recombinant r-Ins$P_3$R-3.

*Heteroligomeric Interactions of r-Ins$P_3$R-3 and X-Ins$P_3$R-1*

Since types 1 and 3 Ins$P_3$R isoforms can form heterotetrameric complexes in cells that coexpress them both (Joseph et al., 1995; Monkawa et al., 1995; Wojcikiewicz and He, 1995; Nucifora et al., 1996), we also considered whether some of the r-Ins$P_3$R-3 channel activities we recorded might be contributed by heterotetramers formed with the *X*-Ins$P_3$R-1. As indicated above, the mean number of Ins$P_3$R channels detected by nuclear patch clamping increased 40-fold after r-Ins$P_3$R-3 cRNA injection. Assuming that Ins$P_3$R channels are tetramers and that they are formed by random, binomial associations of *X*-Ins$P_3$R-1 and r-Ins$P_3$R-3, the large majority (90.3%) of the channels detected in cRNA-injected oocytes are predicted to be homotetrameric r-Ins$P_3$R-3 channels, and most of the rest of the channels (9.4%) are predicted to be composed of one *X*-Ins$P_3$R-1 monomer associated with three r-Ins$P_3$R-3 monomers. To more directly investigate the extent of heterotetramer formation in our studies, we undertook a series of coimmunoprecipitation experiments. Using lysates from oocytes microinjected with r-Ins$P_3$R-3 cRNA, immunoprecipitation of *X*-Ins$P_3$R-1 with Ab-1 coimmunoprecipitated the expressed r-Ins$P_3$R-3, as evidenced by its mobility in SDS-PAGE and detection by immunoblotting with Ab-3 (Fig. 1 F). Two sets of control experiments demonstrated the specificity of the coimmunoprecipitation. First, r-Ins$P_3$R-3 was not detected in similar protocols using uninjected oocytes (Fig. 1, C and D). Second, for both the control and injected oocytes, nonspecific binding to the agarose beads was also evaluated (Fig. 1, C and E). Converse experiments were similarly performed: immunoprecipitation by Ab-3 of r-Ins$P_3$R-3 from cRNA-injected oocyte lysates coimmunoprecipitated *X*-Ins$P_3$R-1 (Fig. 1 J). Again, similar controls, for nonspecific, antibody-independent binding to beads (Fig. 1, G and I), and using uninjected oocyte lysates (Fig. 1, G and H), were performed. These experimental results suggest that the *Xenopus* type 1 and rat type 3 Ins$P_3$R isoforms may form heterotetrameric complexes in oocytes. The amount of r-Ins$P_3$R-3 that coimmunoprecipitated with the *X*-Ins$P_3$R-1 from the pooled lysates of 15 cRNA-injected oocytes (Fig. 1 F) was roughly equivalent to the amount of r-Ins$P_3$R-3 protein present in the lysate of one cRNA-injected oocyte (Fig. 1 B). In control experiments, the amount of *X*-Ins$P_3$R-1 immunoprecipitated by Ab-1 from the pooled lysates of 15 uninjected oocytes and detected by immunoblotting with Ab-1 was over an order of magnitude greater than the amount of *X*-Ins$P_3$R-1 detected by Ab-1 in the lysate of one uninjected oocyte (not shown), indicating an efficiency of immunoprecipitation of *X*-Ins$P_3$R-1 by Ab-1 of $>$67%. Therefore, the coimmunoprecipitation result indicates that $\sim$7–10% of the r-Ins$P_3$R-3 expressed in the cRNA-injected oocytes was involved in heteroligomer formation with the endogenous *X*-Ins$P_3$R-1. This biochemical result compares well with the $\sim$9% predicted from the binomial statistics. The good agreement between these completely independent determinations suggests that $>$90% of the channel activities observed in r-Ins$P_3$R-3–injected oocyte nuclei in the present studies were contributed by homotetramers of r-Ins$P_3$R-3 monomers, and $<$10% of them were contributed by tetramers that contained one *X*-Ins$P_3$R-1 monomer.

*Characterization of the Single-channel Conductance and Gating Properties of r-Ins$P_3$R-3 in Xenopus Oocytes*

Because these results strongly suggested that the channel activities we measured in oocytes expressing r-Ins$P_3$R-3 were overwhelmingly contributed by type 3 homotetramers, we proceeded to use this expression system to characterize the properties of the r-Ins$P_3$R-3 channel. The major rationale for developing this expression system was to determine whether different Ins$P_3$R isoforms have similar or distinct permeation and gating properties when their channel activities are measured in the same physiological membrane system. To facilitate comparisons of the permeation and gating behaviors of the two isoforms, we used conditions that were previously employed to characterize the *X*-Ins$P_3$R-1 in this same nuclear membrane (Mak and Foskett, 1994, 1998). In symmetric KCl solution containing 2.5 mM $Mg^{2+}$, the r-Ins$P_3$R-3 channel has a stable conductance (Fig. 3 A), with a channel current–voltage relation that is nonlinear and asymmetric with respect to the origin, with $I(-V_{app}) = -0.7 \times (V_{app})$, where $V_{app}$ is the applied voltage ($V_{app} > 0$ mV in this equation) (Fig. 3 B). The slope conductance near 0 mV was $\sim$119 pS, increasing to $\sim$360 pS at +50 mV. We previously demonstrated that nonlinearity of the *X*-Ins$P_3$R-1 I-V relation was caused by $Mg^{2+}$ permeation in the channel (Mak and Foskett, 1998). We therefore investigated the I-V relation in the absence of free $Mg^{2+}$. In symmetric KCl solution with 0 mM $Mg^{2+}$, the Ins$P_3$R-3 I-V relation became linear with a conductance of 358 $\pm$ 8 pS (see Fig. 5 B). Thus, $Mg^{2+}$ is a permeant ion blocker, reducing channel conductance and causing rectification of the I-V relation in the r-Ins$P_3$R-3, as it does in the *X*-Ins$P_3$R-1 (Mak and Foskett, 1998). $Mg^{2+}$ also plays an important role in stabilizing the conductance of *X*-Ins$P_3$R-1 channel. A similar role for $Mg^{2+}$ was observed for the

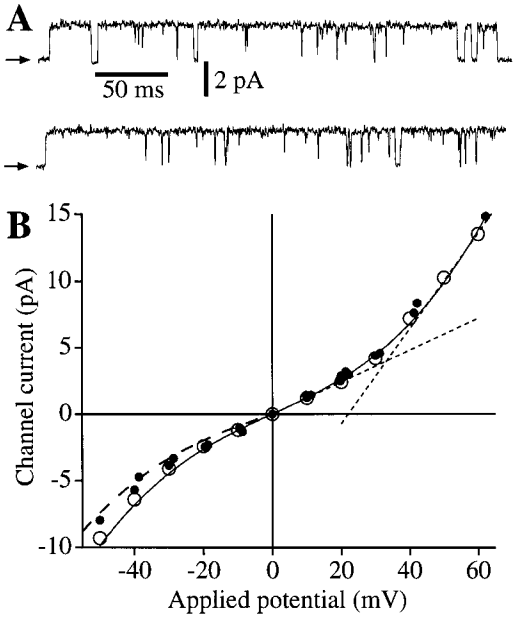


Figure 3. Conductance of the recombinant r-Ins$P_3$R-3 in the nuclear membrane. (A) Typical patch clamp current traces for r-Ins$P_3$R-3 channels in symmetric solutions containing 2.5 mM $Mg^{2+}$ and $[Ca^{2+}]_i$ = 940 nM. (B) I-V relation for the r-Ins$P_3$R-3 (●) in symmetric 2.5 mM $Mg^{2+}$ solutions. Channel currents were averaged from all channel opening and closing events from five current records (over 100 events in each record). SEM bars are smaller than the symbols. I-V relation for the *X*-Ins$P_3$R-1 channels in the same ionic conditions (○) obtained previously (Mak and Foskett, 1998) is also plotted for comparison. Solid curve is a fifth-order odd polynomial [$I = a_1V_{app} + a_3(V_{app})^3 + a_5(V_{app})^5$] fitted to the r-Ins$P_3$R-3 data under positive $V_{app}$. (Dotted line) The slope conductances ($dI/dV$) of 119 pS at 0 mV and 360 pS at 50 mV. Dashed curve: 0.7× the value of the solid curve.

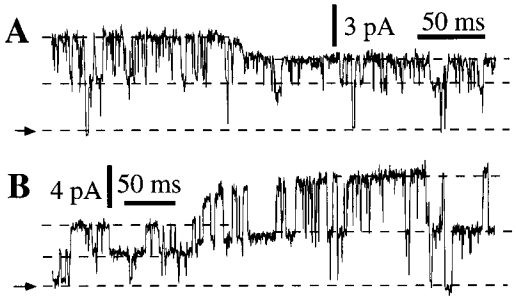


Figure 4. r-Ins$P_3$R-3 channel conductance fluctuates in the absence of $Mg^{2+}$. (A) Current trace from a patch with two Ins$P_3$R-3 channels, one of which had fluctuating conductance, in symmetric solutions containing 0 mM $Mg^{2+}$; $[Ca^{2+}]_i$ = 221 nM. (B) Current trace showing two Ins$P_3$R-3 channels with conductance fluctuating in concert, with 2.5 mM $Mg^{2+}$ on the pipette side and 0 mM $Mg^{2+}$ on the bath side of the channel; $[Ca^{2+}]_i$ = 1,260 nM.

r-Ins$P_3$R-3 channel. Thus, in the absence of $Mg^{2+}$ on both (Fig. 4 A) or just one (B) side of the r-Ins$P_3$R-3 channel, the channel conductance occasionally fluctuated under constant $V_{app}$ during the course of a recording (~2 min), or even during single-channel openings (~10 ms). In patches with multiple channels, their conductances fluctuated independently (Fig. 4 A) or in concert (Fig. 4 B). However, most records showed channels with stable conductances (Fig. 2). To avoid possible effects of channel conductance fluctuations, a voltage ramp protocol (Fig. 5) was used to determine the channel conductance of the r-Ins$P_3$R-3.

Conductance states other than the predominant main (M) state were also observed in either the presence or absence of $Mg^{2+}$. Most noticeably, a small conductance state (S) with conductance ~0.7 that of the M state (Fig. 6 A) was frequently observed (>20% of channel open time). A half (H) conductance state with conductance 0.5 that of state M was observed occasionally (<1% of channel open time) (Fig. 6 B). Besides the normal kinetic mode, the Ins$P_3$R-3 channel was sometimes (<5% of the patches) observed in a "flicker" kinetic mode, in which the channel rapidly alternated between two conductance states ($F_1$ and $F_2$), with conductances ~0.25 and 0.75 that of the M state. Similar flicker kinetics have been observed in the *X*-Ins$P_3$R-1 channel (Mak and Foskett, 1997). The conductance substates (S and H) and flicker kinetic mode were observed in both the presence and absence of $Mg^{2+}$. From statistical considerations based on the frequency of observance of the substate and the probability of detecting heteroligomeric Ins$P_3$R channels, the more frequently observed substate (S) must be a substate of the r-Ins$P_3$R-3 homotetramer, but we cannot ascertain whether the less frequently observed substates (H, $F_1$, and $F_2$) occurred in r-Ins$P_3$R-3 homotetramers or in heterotetramers of *X*-Ins$P_3$R-1 and r-Ins$P_3$R-3.

To determine the ion selectivity of the r-Ins$P_3$R-3 channel, asymmetric ionic conditions were used. In the presence of a $[K^+]$ gradient, in the absence of $Mg^{2+}$, the channel I-V relation is linear (Fig. 7 A) with a reversal potential ($V_{rev}$) of 25.2 mV. Using the Goldman-Hodgkin-Katz (GHK) equations (Hille, 1992), the relative permeabilities of the channel to $K^+$ and $Cl^-$ ($P_K/P_{Cl}$) were calculated to be 4.6. In the absence of $Mg^{2+}$, with a $[Ca^{2+}]$ gradient, the channel I-V relation is nonlinear with $V_{rev}$ = 20.6 mV (Fig. 7 B). Using the GHK equations and the value of $P_K/P_{Cl}$, the relative permeabilities of $Ca^{2+}$ to $K^+$ ($P_{Ca}/P_K$) were determined to be 11. Thus, the channel is a $Ca^{2+}$-selective cation channel.

In all experimental conditions, inactivation of the r-Ins$P_3$R-3 channel was consistently observed. In >90% of the experiments, channel activities terminated within 2 min of formation of the seal. In some of the patches (~10%), the inactivation could be reversed by an increase of 20–40 mV in $V_{app}$. In some patches, the channels could be repeatedly reactivated by jumps in $V_{app}$ before they inactivated irreversibly. These results indicate that the r-Ins$P_3$R-3 channel, like the *X*-Ins$P_3$R-1 (Mak and Foskett, 1997), has two inactivated states: one

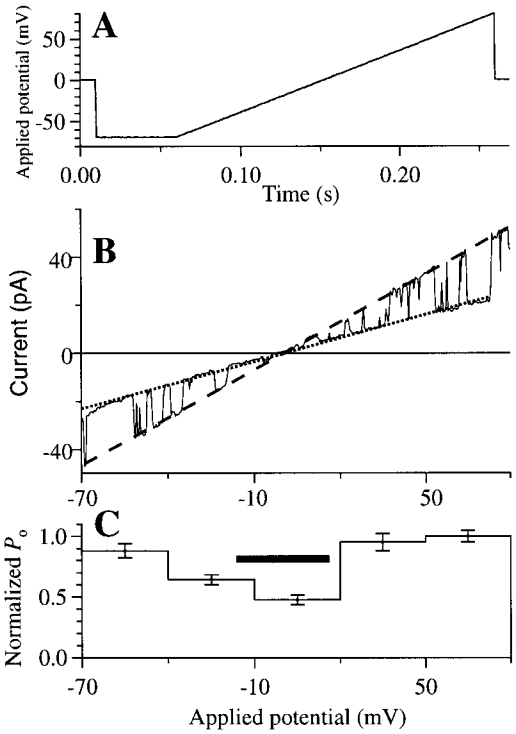


Figure 5. Channel properties of the r-Ins$P_3$R-3 in symmetric 0 mM $Mg^{2+}$ solutions ($[Ca^{2+}]_i$ = 80 nM) under a voltage ramp. (A) The applied voltage ramp used to obtain the current traces. (B) I-V relation obtained from a typical current trace using the voltage ramp. Dotted and dashed lines are the fitted closed and open channel I-V relations, respectively. The channel conductance was evaluated as the difference between the slopes of the two fitted lines. (C) Voltage dependence of $P_o$ of the r-Ins$P_3$R-3 channel. The $P_o$ of the channel observed at various $V_{app}$ during the voltage ramp was binned and averaged over 28 traces to generate the histogram. SEM of the $P_o$ is also plotted. The horizontal bar indicates the voltage range −15 to 15 mV in which channel openings and closings were difficult to discern, so $P_o$ was underestimated.

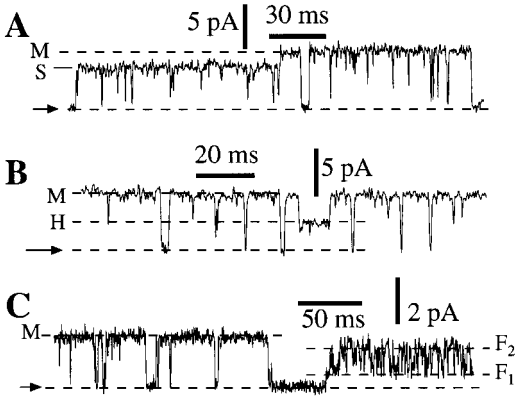


Figure 6. Conductance substates of the Ins$P_3$R channels observed in nuclear patches obtained from r-Ins$P_3$R-3 cRNA-injected oocytes. (A) Current trace showing a transition of an Ins$P_3$R channel from the small (S) conductance state to the main (M) conductance state in symmetric solutions containing 0 mM $Mg^{2+}$; $[Ca^{2+}]_i$ = 1,150 nM. (B) Current trace showing an Ins$P_3$R channel in the rare half (H) conductance state in symmetric solutions containing 0 mM $Mg^{2+}$; $[Ca^{2+}]_i$ = 255 nM. (C) Current trace showing an Ins$P_3$R channel in the normal and flicker kinetic modes in symmetric 2.5 mM $Mg^{2+}$; $[Ca^{2+}]_i$ = 940 nM. $F_1$ and $F_2$ denote the conductance states in the flicker kinetic mode.

($I_{Vdep}$) from which it can be reactivated by a jump in $V_{app}$, and one ($I_{irr}$) from which it cannot exit in the presence of the steady [Ins$P_3$] and $[Ca^{2+}]_i$ conditions used in our experiments.

Analysis of the Ins$P_3$R-3 $P_o$ in experiments in which $V_{app}$ was altered by ramps indicates that $P_o$ between −70 and −40 mV was not significantly different from that between 20 and 80 mV (Fig. 5). The decrease in $P_o$ observed between −40 and 20 mV is likely an artifact caused by the difficulty in discerning channel openings due to the small channel current under those potentials.

*Clustering of the Expressed r-Ins$P_3$R-3*

We previously reported that the *X*-Ins$P_3$R-1 exists in clusters in the outer membrane of the nuclear envelope (Mak and Foskett, 1997). To determine whether channel clustering was also a property of the expressed r-Ins$P_3$R-3, we analyzed the distribution of channel densities among the nuclear patches from cRNA-injected oocytes. The number of channels in each patch was estimated by determining the number of Ins$P_3$R channel current levels observed. Histogram analysis of the distribution of patches exhibiting various numbers of Ins$P_3$R channel current levels was undertaken using the results from 767 nuclear patches (Fig. 8). Analysis of these results and comparisons with the Poisson distribution (Fig. 8) suggests that the expressed r-Ins$P_3$R-3 are not evenly distributed over the surface of the outer nuclear membrane, but are localized in clusters. The similar clustering observed for both the endogenous *X*-Ins$P_3$R-1 and recombinant expressed X-Ins$P_3$R-3 suggests that the ability of the Ins$P_3$R tetramers to associate into clusters is a general property of Ins$P_3$Rs.

*Role of the r-Ins$P_3$R-3 in $Ca^{2+}$ Release-activated Plasma Membrane $Ca^{2+}$ Influx*

Two studies have previously concluded that the r-Ins$P_3$R-3 plays a role in mediating $Ca^{2+}$ flux into the cell across the plasma membrane. In lymphocytes, the r-Ins$P_3$R-3 was localized at or near the plasma membrane in apoptotic cells, and antisense inhibition of its expression diminished apoptosis, presumably by diminishing $Ca^{2+}$ influx (Khan et al., 1996). In *Xenopus* oocytes, expression of r-Ins$P_3$R-3 was without effect on Ins$P_3$-mediated $Ca^{2+}$ release, but enhanced the extent and duration of $Ca^{2+}$ influx activated by Ins$P_3$-induced $Ca^{2+}$ release from intracellular stores (DeLisle et al., 1996). $Ca^{2+}$ influx across the plasma membrane in response to depletion of intracellular $Ca^{2+}$ stores, $Ca^{2+}$-release-activated $Ca^{2+}$ influx (DeLisle et al., 1996) or store-operated $Ca^{2+}$ (SOC) influx (Parekh et al., 1997), has been observed in numerous cell types, but the mechanisms that

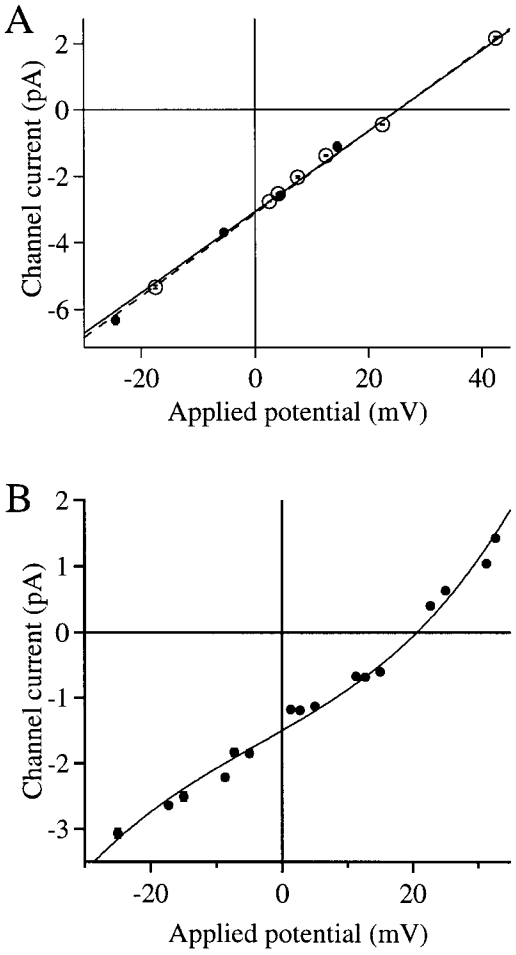


Figure 7. Ion selectivity of the r-Ins$P_3$R-3. (A) The I-V curve of the Ins$P_3$R-3 in the presence of solutions containing asymmetric $K^+$ concentrations. The pipette contained the low $K^+$ solution. The bath solution was the standard 140 mM KCl solution with 0 mM $Mg^{2+}$. $V_{app}$ values were corrected for the liquid junction potential (Neher, 1992) between the asymmetric solutions across the membrane patch. Channel currents were obtained as in Fig. 3. ● are data points for r-Ins$P_3$R-3 fitted with the dashed line, giving $V_{rev}$ = 25.2 ± 0.7 mV. ○ are data points for *X*-Ins$P_3$R-1 fitted with the solid line, giving $V_{rev}$ = 25.3 ± 0.2 mV. (B) The I-V curve of Ins$P_3$R-3 in the presence of a $[Ca^{2+}]$ gradient. The pipette contained the standard 140 mM KCl solution with 0 mM $Mg^{2+}$ and $[Ca^{2+}]_i$ = 24.7 nM. To avoid exposing the oocyte nucleus to high $[Ca^{2+}]$, which interferes with formation of giga-ohm seals (Mak and Foskett, 1994), an excised patch with Ins$P_3$R activities was first obtained from a nucleus in the standard 140 mM KCl solution (0 mM $Mg^{2+}$). The bath solution was then replaced with the high $Ca^{2+}$ solution by perfusion. $V_{app}$ values were corrected for liquid junction potential (Neher, 1992) between the asymmetric solutions across the membrane patch. Channel currents were obtained as in Fig. 3. The solid curve is a fifth order polynomial fitted to the data points, giving $V_{rev}$ = 20.6 ± 0.5 mV.

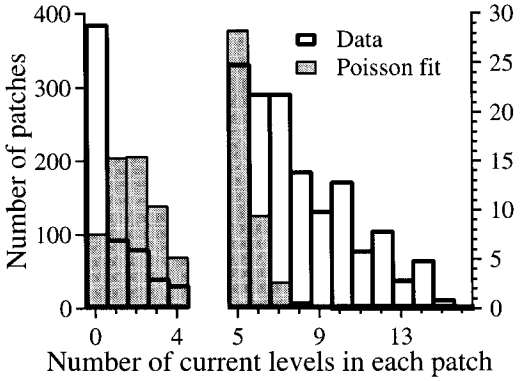


Figure 8. Histogram analysis of number of current levels (abscissa) observed in 767 nuclear patch clamp experiments using isolated nuclei from r-Ins$P_3$R-3 cRNA-injected oocytes (unshaded histogram with thick outline). Also plotted is the Poisson distribution (shaded histogram with thin outline) with the same mean current level number ($\langle n \rangle$ = 2.016) per patch. Note the different y-axis scales used in the histogram. The number of patches containing a large number of channels (6–15) exceeds that predicted from Poisson statistics, suggesting that the recombinant type 3 Ins$P_3$R channel localizes in clusters.

couple the state of $Ca^{2+}$ filling of the internal stores with the plasma membrane influx pathway has remained obscure. In a recent review, Putney (1997) suggested, based in part on the above studies, that the Ins$P_3$R-3 may contribute to, or in fact be, a plasma membrane $Ca^{2+}$ influx pathway involved in this process. The Ins$P_3$R-3 has been localized near or at the plasma membrane in several cell types (Maranto, 1994; Nathanson et al., 1994; Lee et al., 1997; Yule et al., 1997). Our patch-clamp results suggest that the Ins$P_3$R-3 expressed in oocytes localizes to the outer membrane of the nuclear envelope, and presumably to the ER as well, although they do not exclude a plasma membrane localization. We therefore examined whether expression of r-Ins$P_3$R-3 in *Xenopus* oocytes conferred an enhanced SOC influx in this cell type. We employed two different published TEV protocols to examine SOC influx in oocytes injected with r-Ins$P_3$R-3 cRNA. In one (Hartzell, 1996), $[Ca^{2+}]_i$ was monitored by recording the magnitude of the $Ca^{2+}$-activated $Cl^-$ current using TEV (Fig. 9 A). Ins$P_3$ was injected into the cytoplasm to activate the Ins$P_3$R, as evidenced by a rapid increase of the $Ca^{2+}$-activated $Cl^-$ current ($\Delta G^{Cl}_{IP3}$). After depletion of the internal $Ca^{2+}$ stores, as evidenced by the lack of $Cl^-$ current responses to repeated subsequent Ins$P_3$ injections (Fig. 9 A), the magnitude of $Ca^{2+}$ influx was monitored indirectly by the $Cl^-$ current response ($\Delta G^{Cl}_{SOC}$) to an acute step increase in $[Ca^{2+}]$ in the bathing solution. Comparison of responses of control ($n$ = 14 oocytes from five different batches) and r-Ins$P_3$R-3–expressing ($n$ = 21 oocytes from the same five batches) oocytes revealed no significant difference in the magnitudes of $\Delta G^{Cl}_{IP3}$ (24.2 ± 2.6 μS, mean ± SEM, for controls oocytes; 22.9 ± 3.8 μS for r-Ins$P_3$R-3 expressing oocytes; $P$ = 0.77) or $\Delta G^{Cl}_{SOC}$ (26.6 ± 5.0 μS for control oocytes; 20.2 ± 3.9 μS for expressing oocytes; $P$ = 0.32). Functional expression of the r-Ins$P_3$R-3 in these experiments was verified by high probability of detect-

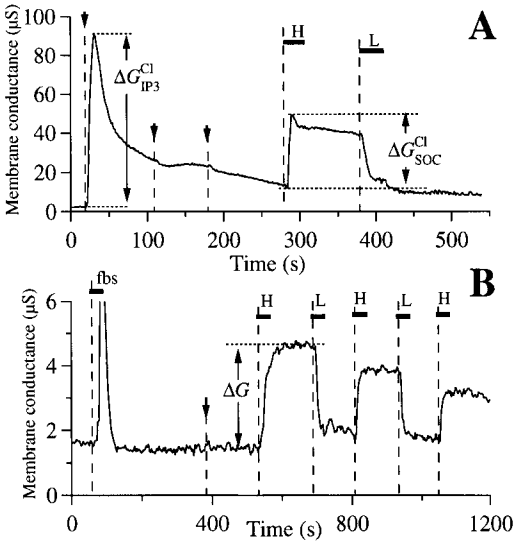


Figure 9. Store-operated calcium influx across the oocyte plasma membrane. Whole-cell transmembrane conductance of r-Ins$P_3$R-3 cRNA-injected *Xenopus* oocytes was recorded in two types of TEV experiments. (A) $Ca^{2+}$-activated plasma membrane $Cl^-$ channel current after microinjection of Ins$P_3$ in various bathing solutions. Arrows indicate injections of Ins$P_3$ into the oocyte. Horizontal bars indicate exchange of bathing solution by perfusion with a high $Ca^{2+}$ solution HCa96 (H) or a low $Ca^{2+}$ solution LCa96 (L). The magnitudes of the changes in membrane conductance due to plasma membrane $Ca^{2+}$-activated $Cl^-$ current response to Ins$P_3$ injection ($\Delta G^{Cl}_{IP3}$) and due to $Ca^{2+}$ influx through store-operated $Ca^{2+}$ channels ($\Delta G^{Cl}_{SOC}$) are marked. (B) Store-operated $Ca^{2+}$ currents after activation of Ins$P_3$R in various bathing solutions. Horizontal bars indicate exchange of bathing solution with high $Ca^{2+}$ solution HCa96 (H), low $Ca^{2+}$ solution LCa96 (L), and low $Ca^{2+}$ LCa96 containing 1:100 fetal bovine serum (fbs). Arrow indicates microinjection of BAPTA. Magnitude of changes in membrane conductance due to $Ca^{2+}$ influx through store-operated $Ca^{2+}$ channels ($\Delta G$) is indicated.

ing Ins$P_3$R channel activities during subsequent patch clamping of nuclei from the oocytes used in the TEV experiments. Thus, we were unable to reproduce the results of DeLisle et al. (1996). A second protocol (Yao and Tsien, 1997) was also employed (Fig. 9 B). Membrane conductance ($\Delta G$) due to the SOC influx pathway was not different ($P = 0.98$) in control ($n = 3$, mean = 2.4 ± 0.5 μS) compared with Ins$P_3$R-3–expressing oocytes ($n = 4$, mean = 2.4 ± 0.3 μS). These studies also do not support the hypothesis that Ins$P_3$R-3 plays a rate-limiting role in mediating SOC influx.

## DISCUSSION

In this report, we have demonstrated the functional expression of the type 3 isoform of the Ins$P_3$R, a widely expressed isoform in mammalian tissues, in a system which enabled recording of its single-channel activity in its normal ER membrane environment. Patch-clamp electrophysiology of the r-Ins$P_3$R-3 in the *Xenopus* nuclear envelope represents the first description of the permeation and gating properties of the recombinant type 3 Ins$P_3$R.

### *Use of Xenopus oocytes for Expression of Recombinant ER-localized Ion Channels*

A major impediment to understanding $[Ca^{2+}]_i$ signaling has been the lack of robust systems to study the gating and permeation properties of the Ins$P_3$Rs. As intracellular ion channels, they have been considered inaccessible to patch-clamp electrophysiological approaches. Most studies have therefore employed indirect measurements that can only infer channel activity, and which report the responses from populations of channels containing multiple receptor isoforms. Some recent studies have employed cultured cells that express predominantly one isoform (Kaznacheyeva et al., 1998), but these studies continue to suffer from the problems of receptor heterogeneity as well as the inability to understand $Ca^{2+}$ release properties within the context of relevant ion channel parameters, including gating and permeation measures. As with other intracellular ion channels, reconstitution of the Ins$P_3$R into planar lipid membranes has been used to record the single-channel properties (Bezprozvanny et al., 1991, 1994; Watras et al., 1991; Bezprozvanny and Ehrlich, 1994; Perez et al., 1997; Ramos-Franco et al., 1998b). Two strategies have been employed. In the first, membranes from cerebellum (Bezprozvanny et al., 1991; Watras et al., 1991), heart (Perez et al., 1997; Ramos-Franco et al., 1998b) and RIN (Hagar et al., 1998) cells have been used, because of their high expression levels of Ins$P_3$R-1, Ins$P_3$R-2, and Ins$P_3$R-3, respectively. In the second, membranes were obtained from cells engineered to over-express recombinant Ins$P_3$R: Ins$P_3$R-1 in HEK-293 cells (Kaznacheyeva et al., 1998), and wild-type and mutant Ins$P_3$R-1 in COS-1 cells (Ramos-Franco et al., 1998a, 1999). The latter approach has the potential advantage of enabling structure–function studies of the protein. However, the relevance of channel behavior in vitro in artificial bilayers for in vivo behavior in ER membrane remains unknown.

Since the ER is continuous with the outer membrane of the nuclear envelope (Dingwall and Laskey, 1992), we reasoned that ER-localized ion channels would also be present in the nuclear envelope outer membrane, and that single-channel properties of the Ins$P_3$R in its native membrane environment could be examined by patch clamping isolated nuclei. Formation of seals with gigaohm resistance on the outer nuclear membrane, a prerequisite for studying single ion channel activity, was achieved with high frequency despite the high density of nuclear pores in the *Xenopus* oocyte nuclear envelope (Mak and Foskett, 1994, 1997, 1998; Stehno-Bittel

et al., 1995). We have used this system to study the endogenous $InsP_3R$ channel (Mak and Foskett, 1994, 1997, 1998). The oocyte expresses only a single $InsP_3R$ isoform (type 1) and lacks other (e.g., ryanodine receptor) $Ca^{2+}$ release channels (Parys et al., 1992). Because the *Xenopus* oocyte has been used extensively to express functional recombinant mammalian plasma membrane ion channels, we reasoned that this system, combined with nuclear patch clamping, would enable the recording of recombinant $InsP_3R$ channel activities in their native ER membrane. The results presented here demonstrate that this is the case. The major potential complication in this approach is that the oocyte nucleus may not present a null background for expression of recombinant channels, due to the presence of endogenous $InsP_3R$ channels. Nevertheless, we have been able to minimize this problem by using batches of oocytes in which endogenous channel activity could not be detected by nuclear patch clamping. The basis for frog-to-frog variability in our ability to record the endogenous $InsP_3R$-1 in oocyte nuclei is not clear, although we believe there is a seasonal component, in addition to others. It has not been uncommon in our experience to examine oocytes from many different frogs over the course of a couple of months and not record the endogenous channel in any of hundreds of nuclear patches. In preliminary experiments, we determined that the lack of detectable endogenous $InsP_3R$ channel activities immediately after oocyte isolation did not reverse over time in culture. Therefore, in the present study, we selected "null backgrounds" for expression of the type 3 channel by performing a day of screening patch-clamp experiments to ascertain that the endogenous channel was minimally present in the nuclei of the oocytes used for injection. In contrast, in oocytes injected to express the r-$InsP_3R$-3, the number of $InsP_3R$ channels observed in nuclear patches was dramatically increased by nearly 40-fold. Based purely on statistical probabilities, there is therefore little likelihood of contamination of the data by $InsP_3R$-1 homotetramers in our studies. Nevertheless, it remained possible that expression of the recombinant r-$InsP_3R$-3 might have upregulated the endogenous *Xenopus* type 1 channel. However, Western blot analysis revealed that the amount of *X*-$InsP_3R$-1 remained constant in both control and injected oocytes. These results strongly indicate that channel activities recorded in the r-$InsP_3R$-3–expressing oocytes were contributed by the recombinant channels. Assuming random association of monomers to form tetrameric functional channels, binomial statistics indicates that >90% of the recorded channels in these studies are contributed by r-$InsP_3R$-3 homotetramers, whereas <10% of recorded channels represent tetramers containing three type 3 monomers with one type 1 monomer. The validity of these statistically based conclusions was evaluated in coimmunoprecipitation experiments using control and injected oocytes. We determined that the endogenous type 1 $InsP_3R$ coimmunoprecipitated with the expressed recombinant type 3 $InsP_3R$. Coimmunoprecipitation of different $InsP_3R$ isoforms has previously been interpreted to indicate heterotetramer formation (Joseph et al., 1995; Monkawa et al., 1995; Wojcikiewicz and He, 1995; Nucifora et al., 1996). Of note, quantification of the amounts of coimmunoprecipitated protein suggests that <10% of the expressed recombinant type 3 channels were associated with the endogenous *Xenopus* channels. This biochemical result is in good agreement with the extent of isoform associations predicted from patch clamp statistics. Thus, the combined patch-clamp results and their statistical analysis, strongly corroborated by biochemical evidence, indicates that a large majority (>90%) of the patch-clamp data in the present experiments were contributed by r-$InsP_3R$-3 homotetramers.

The similar permeation properties of the expressed and endogenous channels, as we have now defined in the present work, necessitated this exhaustive approach to ensure the identities of the recorded channels. Nevertheless, we discovered that the gating properties of the two channels can be used to distinguish them, under conditions of low cytoplasmic $Ca^{2+}$ concentration. Thus, whereas the $P_o$ of both channels is equivalent ($\sim$0.8) when cytoplasmic $Ca^{2+}$ concentration is 1 $\mu$M (Mak et al., 1998, and this study), the $P_o$ of the type 3 channel is considerably higher than that of the endogenous channel when cytoplasmic $Ca^{2+}$ concentration is $\sim$80 nM. Although more detailed studies are required to define the $Ca^{2+}$ concentration dependence of $InsP_3R$-3 gating, this ability to distinguish the expressed channels from the endogenous ones provides additional strong support for the validity of this approach. Parenthetically, our results suggest that high $[Ca^{2+}]_i$ (>50 $\mu$M) inhibits the type 3 channel similarly to the endogenous type 1 channel. The conclusion that high $[Ca^{2+}]_i$ inhibition does not distinguish the types 1 and 3 channels contrasts with that reached in a bilayer study using microsomes isolated from a cell type expressing predominately the type 3 isoform (Hagar et al., 1998). The bases for the discrepant results in the two studies are not known. In the present study, homotetramers of the type 3 isoform were recorded, as discussed above, in a native membrane environment, whereas the bilayer study recorded channels of unknown isoform composition in artificial membranes after reconstitution. Further, more detailed studies are in progress to determine the complete $[Ca^{2+}]_i$ dependence of $InsP_3R$-3 gating, which may help to resolve these discrepancies. Our success in the approach described in the current work suggests that it will now be possible to express and record the properties of mutant $InsP_3Rs$ in the ER in

future studies of structure–function relationships, and that it will be useful for studying other ER-localized ion channels, whether localized there normally or as a result of natural or engineered mutations. Of note, however, it may be necessary to perform a similar series of control experiments for each mutant expressed to ensure that the system behaves as we have described for the wild-type r-Ins$P_3$R-3.

### *Permeation and Gating Properties of the r-Ins$P_3$R-3 and X-Ins$P_3$R-1 from Nuclear Patch Clamp Studies*

We examined the basic channel properties of the r-Ins$P_3$R-3 and found that they are remarkably similar, particularly in view of both the isoform and species differences, to those of the *X*-Ins$P_3$R-1 in the same membrane system.

In terms of permeation, both channels are relatively nonselective cation channels: $P_K/P_{Cl}$ is 4.6 for both *X*-Ins$P_3$R-1 and r-Ins$P_3$R-3 (Fig. 3). Our previously reported value of $P_K/P_{Cl}$ for *X*-Ins$P_3$R-1 (Mak and Foskett, 1994) was overestimated because $Mg^{2+}$ present in the pipette and bath solutions in those experiments caused nonlinearity in the I-V relation of the channel (Mak and Foskett, 1998) and the use of the Goldman-Hodgkin-Katz equation to fit the experimental I-V relation and determine $V_{rev}$ was inappropriate. Applying this revised value of $P_K/P_{Cl}$, $P_{Ca}$:$P_{Ba}$:$P_{Mg}$:$P_K$ for *X*-Ins$P_3$R-1 is calculated to be 12.7:8.6:6.4:1 based on $V_{rev}$ measured in Mak and Foskett (1998). Thus, the values for $P_{Ca}/P_K$ for the two channels are very similar (12.7 for *X*-I$P_3$R-1; 11.0 for r-I$P_3$R-3). In both channels, the I-V relation is linear in the absence of $Mg^{2+}$, and the absence of $Mg^{2+}$ is associated with occasional conductance fluctuations under constant $V_{app}$ during the course of a recording (~2 min), or even during single-channel openings (~10 ms). The conductances of both channels are stabilized and become rectified as [$Mg^{2+}$] is increased on either side of the membrane. $Mg^{2+}$ decreases single-channel conductance of both channels to a similar extent (Fig. 3 B), due to permeant ion block (Mak and Foskett, 1998).

Both channels display conductance states of S and H (Mak and Foskett, 1994, 1998), while both gate primarily in the main M state, though the frequency of finding the channel in state S was much higher in the r-Ins$P_3$R-3. Both channels undergo two forms of Ins$P_3$-dependent inactivation: one (relatively rare) that can be reversed by momentarily jumping the applied potential to 60 mV, and one (all channels) that is apparently irreversible under our steady state experimental conditions. Although we have not quantified the kinetics of irreversible inactivation for the Ins$P_3$R-3, it is our general impression that they are similar to those of the *X*-Ins$P_3$R-1 (time constant ~25 s) (Mak and Foskett, 1997). Both channels displayed flicker kinetics, although this was observed less frequently for the type 3 channel, and the relative values of the two flicker state conductances is the same for both receptors (Mak and Foskett, 1997).

A difference between the two types of Ins$P_3$R is their voltage dependencies. Whereas $P_o$ of the *X*-Ins$P_3$R-1 was reduced by an increase in $V_{app}$ (Mak and Foskett, 1997), the $P_o$ of r-Ins$P_3$R-3 showed little voltage dependence, or was even slightly activated by high magnitude $V_{app}$ regardless of polarity (this study).

### *Comparison of the Permeation and Gating Properties of Different Ins$P_3$R Isoforms*

Our results suggest that the permeation pathways and gating mechanisms are remarkably similar between the types 1 and 3 Ins$P_3$R channels. Including the present data, single-channel recordings have now been obtained for all three known Ins$P_3$R isoforms. A side-by-side comparison of the bovine type 1 and ferret type 2 receptors in proteoliposome-fused bilayers revealed that their conductance properties were nearly identical (Ramos-Franco et al., 1998b). Taken together with our results, these data indicate that the permeation pathways in all three Ins$P_3$R channels are very similar. This result has implications for the structural properties of the conduction pores in the three isoforms. Of note, there is conservation among the isoforms of amino acid sequences in regions that are speculated to be involved in pore formation (Yamamoto-Hino et al., 1994).

Nevertheless, some differences have been reported in the gating behaviors of the three channel isoforms, although it is not clear whether they reflect isoform differences or are due to unknown variables associated with different experimental protocols. The type 1 channel has been studied in different systems, including reconstitution of cerebellar membranes (Bezprozvanny et al., 1991, 1994; Watras et al., 1991; Bezprozvanny and Ehrlich, 1994) and proteoliposomes (Kaznacheyeva et al., 1998) and patch clamp of the *Xenopus* nuclear envelope (Mak and Foskett, 1994, 1997, 1998; Stehno-Bittel et al., 1995), whereas the type 2 channel has been studied using reconstituted proteoliposomes (Perez et al., 1997; Ramos-Franco et al., 1998b), and the type 3 channel has been studied by reconstitution (Hagar et al., 1998) and nuclear patch clamping (this study). Furthermore, the channels have come from different species (type 1: canine, bovine, *Xenopus*, rat; type 2: ferret; type 3: rat). Reconstituted receptors in bilayers are distinguished by a maximum $P_o$ of ~0.7 for the type 2 channel vs. ~0.2 for the type 1 isoform (Ramos-Franco et al., 1998b) and ~0.05 for the type 3 channel (Hagar et al., 1998). These differences were interpreted as reflecting isoform differences (Ramos-Franco et al., 1998b), but the fact that the maximum $P_o$ observed for both the *X*-Ins$P_3$R-1 (Mak et al., 1998) and r-Ins$P_3$R-3 (Figs. 2 and 3 A) was nearly identical (~0.8) suggests that isoform differences may not be particularly rele-

vant. Indeed, other factors may be more important since the gating properties reported for the type 1 receptor from *Xenopus* in the nuclear membrane and rat/canine in artificial bilayers are quite distinct, and those for the rat type 3 channel in endoplasmic reticulum (this study) versus bilayers (Hagar et al., 1998) are similarly distinct. The *X*-Ins$P_3$R-1 studied by nuclear patch clamping (Mak and Foskett, 1997) has a much higher maximum $P_o$, longer open time constant, and prominence of a different conductance state compared with the r-Ins$P_3$R-1 studied by reconstitution into lipid bilayers (Watras et al., 1991), and demonstrates inactivation and voltage-dependent and flicker kinetics that have not been observed in the r-Ins$P_3$R-1 studies. Similarly, the r-Ins$P_3$R-3 studied by nuclear patch clamping (this study) has a maximum $P_o$ of 80% vs. 5% for the reconstituted channel in bilayers (Hagar et al., 1998), and also displays the same rich repertoire of gating behaviors not observed in the bilayer studies. It is possible that the Ins$P_3$R channel properties are sensitive to the membrane isolation, solubilization, and reconstitution protocols employed in bilayer studies. This explanation cannot, however, account for the differences observed between the types 1 and 2 receptors using similar reconstitution protocols (Ramos-Franco et al., 1998b) unless there is a differential sensitivity among isoforms or tissue sources to these procedures. In preliminary studies, we expressed the r-Ins$P_3$R-1 in *Xenopus* oocytes and patch clamped the oocyte nuclear membrane, and have observed gating properties that are similar to those of the *X*-Ins$P_3$R-1 and r-Ins$P_3$R-3 in the same membrane (our unpublished data). This result suggests that the channels in the same native membrane environment gate similarly, and that the channel properties are sensitive to the membrane environment or to the protocols involved in reconstitution. Although further single-channel permeation and gating determinations are necessary to resolve these issues, the data available to date suggest that the three receptor isoforms share quite similar permeation properties. Taken together, these results therefore suggest that if cellular expression of multiple Ins$P_3$R isoforms is a mechanism to modify the temporal and spatial features of $[Ca^{2+}]_i$ signals, then it must be achieved by isoform-specific regulation or localization of various types of Ins$P_3$Rs that have relatively similar $Ca^{2+}$ permeation properties.

We thank Dr. Graeme I. Bell and Dr. Bill Skach for providing expression vectors.

This work was supported by grants to J.K. Foskett from the National Institutes of Health (NIH) (GM56328) and the Department of Defense, and to S.K. Joseph from the NIH (DK34804).

*Submitted: 10 November 1999*
*Revised: 7 January 2000*
*Accepted: 18 January 2000*
*Released online: 14 February 2000*

REFERENCES

Amundson, J., and D. Clapham. 1993. Calcium waves. *Curr. Opin. Neurobiol.* 3:375–382.

Atri, A., J. Amundson, D. Clapham, and J. Sneyd. 1993. A single-pool model for intracellular calcium oscillations and waves in the *Xenopus laevis* oocyte. *Biophys. J.* 65:1727–1739.

Berridge, M.J. 1993. Inositol trisphosphate and calcium signalling. *Nature.* 361:315–325.

Berridge, M.J. 1995. Inositol trisphosphate and calcium signaling. *Ann. NY Acad. Sci.* 766:31–43.

Bezprozvanny, I., J. Watras, and B.E. Ehrlich. 1991. Bell-shaped calcium-response curves of Ins(1,4,5)$P_3$- and calcium-gated channels from endoplasmic reticulum of cerebellum. *Nature.* 351: 751–754.

Bezprozvanny, I., S. Bezprozvannaya, and B.E. Ehrlich. 1994. Caffeine-induced inhibition of inositol(1,4,5)-trisphosphate–gated calcium channels from cerebellum. *Mol. Biol. Cell.* 5:97–103.

Bezprozvanny, I., and B.E. Ehrlich. 1994. Inositol (1,4,5)-trisphosphate (Ins$P_3$)–gated Ca channels from cerebellum: conduction properties for divalent cations and regulation by intraluminal calcium. *J. Gen. Physiol.* 104:821–856.

Bezprozvanny, I., and B.E. Ehrlich. 1995. The inositol 1,4,5-trisphosphate (Ins$P_3$) receptor. *J. Membr. Biol.* 145:205–216.

Blondel, O., J. Takeda, H. Janssen, S. Seino, and G.I. Bell. 1993. Sequence and functional characterization of a third inositol trisphosphate receptor subtype, $IP_3$R-3, expressed in pancreatic islets, kidney, gastrointestinal tract, and other tissues. *J. Biol. Chem.* 268:11356–11363.

Boitano, S., E.R. Dirksen, and M.J. Sanderson. 1992. Intercellular propagation of calcium waves mediated by inositol trisphosphate. *Science.* 258:292–295.

Bootman, M.D., and M.J. Berridge. 1995. The elemental principles of calcium signaling. *Cell.* 83:675–678.

Bush, K.T., R.O. Stuart, S.-H. Li, L.A. Moura, A.H. Sharp, C.A. Ross, and S.K. Nigam. 1994. Epithelial inositol 1,4,5-trisphosphate receptors. Multiplicity of localization, solubility, and isoforms. *J. Biol. Chem.* 269:23694–23699.

Clapham, D.E. 1995. Calcium signaling. *Cell.* 80:259–268.

Dal Santo, P., M.A. Logan, A.D. Chisholm, and E.M. Jorgensen. 1999. The inositol trisphosphate receptor regulates a 50-second behavioral rhythm in *C-elegans*. *Cell.* 98:757–767.

Danoff, S.K., C.D. Ferris, C. Donath, G. Fischer, S. Munemitsu, S. Ullrich, S.H. Snyder, and C.A. Ross. 1991. Inositol 1,4,5-trisphosphate receptors: distinct neuronal and nonneuronal forms generated by alternative splicing differ in phosphorylation. *Proc. Natl. Acad. Sci. USA.* 88:2951–2955.

De Smedt, H., L. Missiaen, J.B. Parys, M.D. Bootman, L. Mertens, L. Van den Bosch, and R. Casteels. 1994. Determination of relative amounts of inositol trisphosphate receptor mRNA isoforms by ratio polymerase chain reaction. *J. Biol. Chem.* 269:21691–21698.

De Smedt, H., L. Missiaen, J.B. Parys, R.H. Henning, I. Sienaert, S. Vanlingen, A. Gijsens, B. Himpens, and R. Casteels. 1997. Isoform diversity of the inositol trisphosphate receptor in cell types of mouse origin. *Biochem. J.* 322:575–583.

DeLisle, S., O. Blondel, F.J. Longo, W.E. Schnabel, G.I. Bell, and M.J. Welsh. 1996. Expression of inositol 1,4,5-trisphosphate receptors changes the $Ca^{2+}$ signal of *Xenopus* oocytes. *Am. J. Physiol. Cell Physiol.* 270:C1255–C1261.

Dingwall, C., and R. Laskey. 1992. The nuclear membrane. *Science.* 258:942–947.

Ferris, C.D., R.L. Huganir, S. Supattapone, and S.H. Snyder. 1989. Purified inositol 1,4,5-trisphosphate receptor mediates calcium flux in reconstituted lipid vesicles. *Nature.* 342:87–89.

Ferris, C.D., and S.H. Snyder. 1992. Inositol phosphate receptors

and calcium disposition in the brain. *J. Neurosci.* 12:1567–1574.

Fujino, I., N. Yamada, A. Miyawaki, M. Hasegawa, T. Furuichi, and K. Mikoshiba. 1995. Differential expression of type 2 and type 3 inositol 1,4,5-trisphosphate receptor mRNAs in various mouse tissues: in situ hybridization study. *Cell Tissue Res.* 280:201–210.

Furuichi, T., S. Yoshikawa, A. Miyawaki, K. Wada, N. Maeda, and K. Mikoshiba. 1989. Primary structure and functional expression of the inositol 1,4,5-trisphosphate-binding protein $P_{400}$. *Nature.* 342: 32–38.

Furuichi, T., K. Kohda, A. Miyawaki, and K. Mikoshiba. 1994. Intracellular channels. *Curr. Opin. Neurobiol.* 4:294–303.

Furuichi, T., and K. Mikoshiba. 1995. Inositol 1,4,5-trisphosphate receptor-mediated $Ca^{2+}$ signaling in the brain. *J. Neurochem.* 64: 953–960.

Goldin, A.L. 1992. Maintenance of *Xenopus laevis* and oocyte injection. *Methods Enzymol.* 207:266–278.

Hagar, R.E., A.D. Burgstahler, M.H. Nathanson, and B.E. Ehrlich. 1998. Type III $InsP_3$ receptor channel stays open in the presence of increased calcium. *Nature.* 396:81–84.

Hartzell, H.C. 1996. Activation of different Cl currents in *Xenopus* oocytes by Ca liberated from stores and by capacitative Ca influx. *J. Gen. Physiol.* 108:157–175.

Hille, B. 1992. Ionic Channels of Excitable Membranes. Sinauer Associates, Inc., Sunderland, MA. 341–348.

Honda, Z., T. Takano, N. Hirose, T. Suzuki, A. Muto, S. Kume, K. Mikoshiba, K. Itoh, and T. Shimizu. 1995. Gq pathway desensitizes chemotactic receptor-induced calcium signaling via inositol trisphosphate receptor down-regulation. *J. Biol. Chem.* 270:4840–4844.

Jiang, Q.S., D. Mak, S. Devidas, E.M. Schwiebert, A. Bragin, Y. Zhang, W.R. Skach, W.B. Guggino, J.K. Foskett, and F. Engelhardt. 1998. Cystic fibrosis transmembrane conductance regulator-associated ATP release is controlled by a chloride sensor. *J. Cell Biol.* 143:645–657.

Joseph, S.K., and S. Samanta. 1993. Detergent solubility of the inositol trisphosphate receptor in rat brain membranes. Evidence for association of the receptor with ankyrin. *J. Biol. Chem.* 268:6477–6486.

Joseph, S.K. 1995. The inositol trisphosphate receptor family. *Cell Signal.* 8:1–7.

Joseph, S.K., C. Lin, S. Pierson, A.P. Thomas, and A.R. Maranto. 1995. Heteroligomers of type-I and type-III inositol trisphosphate receptors in WB rat liver epithelial cells. *J. Biol. Chem.* 270:23310–23316.

Kaftan, E.J., B.E. Ehrlich, and J. Watras. 1997. Inositol 1,4,5-trisphosphate ($InsP_3$) and calcium interact to increase the dynamic range of $InsP_3$ receptor-dependent calcium signaling. *J. Gen. Physiol.* 110: 529–538.

Kaznacheyeva, E., V.D. Lupu, and I. Bezprozvanny. 1998. Single-channel properties of inositol (1,4,5)-trisphosphate receptor heterologously expressed in HEK-293 cells. *J. Gen. Physiol.* 111:847–856.

Khan, A.A., M.J. Soloski, A.H. Sharp, G. Schilling, D.M. Sabatini, S.H. Li, C.A. Ross, and S.H. Snyder. 1996. Lymphocyte apoptosis: mediation by increased type 3 inositol 1,4,5-trisphosphate receptor. *Science.* 273:503–507.

Kume, S., A. Muto, J. Aruga, T. Nakagawa, T. Michikawa, T. Furuichi, S. Nakade, H. Okano, and K. Mikoshiba. 1993. The *Xenopus* $IP_3$ receptor: structure, function, and localization in oocytes and eggs. *Cell.* 73:555–570.

Lechleiter, J.D., and D.E. Clapham. 1992. Molecular mechanisms of intracellular calcium excitability in *X. laevis* oocytes. *Cell.* 69:283–294.

Lee, M.G., X. Xu, W.Z. Zeng, J. Diaz, R.J.H. Wojcikiewicz, T.H. Kuo, F. Wuytack, L. Racymaekers, and S. Muallem. 1997. Polarized expression of $Ca^{2+}$ channels in pancreatic and salivary gland cells—correlation with initiation and propagation of $[Ca^{2+}]_i$ waves. *J. Biol. Chem.* 272:15765–15770.

Maeda, N., T. Kawasaki, S. Nakade, N. Yokota, T. Taguchi, M. Kasai, and K. Mikoshiba. 1991. Structural and functional characterization of inositol 1,4,5-trisphosphate receptor channel from mouse cerebellum. *J. Biol. Chem.* 266:1109–1116.

Magnusson, A., L.S. Haug, S.I. Walaas, and A.C. Ostvold. 1993. Calcium-induced degradation of the inositol (1,4,5)-trisphosphate receptor/$Ca^{2+}$-channel. *FEBS Lett.* 323:229–232.

Mak, D.-O.D., and J.K. Foskett. 1994. Single-channel inositol 1,4,5-trisphosphate receptor currents revealed by patch clamp of isolated *Xenopus* oocyte nuclei. *J. Biol. Chem.* 269:29375–29378.

Mak, D.-O.D., and J.K. Foskett. 1997. Single-channel kinetics, inactivation, and spatial distribution of inositol trisphosphate ($IP_3$) receptors in *Xenopus* oocyte nucleus. *J. Gen. Physiol.* 109:571–587.

Mak, D.-O.D., and J.K. Foskett. 1998. Effects of divalent cations on single-channel conduction properties of *Xenopus* $IP_3$ receptor. *Am. J. Physiol.* 275:C179–C188.

Mak, D.-O.D., S. McBride, and J.K. Foskett. 1998. Inositol 1,4,5-trisphosphate activation of inositol trisphosphate receptor $Ca^{2+}$ channel by ligand tuning of $Ca^{2+}$ inhibition. *Proc. Natl. Acad. Sci. USA.* 95:15821–15825.

Maranto, A.R. 1994. Primary structure, ligand binding, and localization of the human type 3 inositol 1,4,5-trisphosphate receptor expressed in intestinal epithelium. *J. Biol. Chem.* 269:1222–1230.

Mignery, G.A., T.C. Sudhof, K. Takei, and P. De Camilli. 1989. Putative receptor for inositol 1,4,5-trisphosphate similar to ryanodine receptor. *Nature.* 342:192–195.

Miledi, R., and I. Parker. 1989. Latencies of membrane currents evoked in *Xenopus* oocytes by receptor activation, inositol trisphosphate and calcium. *J. Physiol.* 415:189–210.

Monkawa, T., A. Miyawaki, T. Sugiyama, H. Yoneshima, M. Yamamoto-Hino, T. Furuichi, T. Saruta, M. Hasegawa, and K. Mikoshiba. 1995. Heterotetrameric complex formation of inositol 1,4,5-trisphosphate receptor subunits. *J. Biol. Chem.* 270:14700–14704.

Nakagawa, T., H. Okano, T. Furuichi, J. Aruga, and K. Mikoshiba. 1991. The subtypes of the mouse inositol 1,4,5-trisphosphate receptor are expressed in a tissue-specific and developmentally-specific manner. *Proc. Natl. Acad. Sci. USA.* 88:6244–6248.

Nathanson, M.H., M.B. Fallon, P.J. Padfield, and A.R. Maranto. 1994. Localization of the type 3 inositol 1,4,5-trisphosphate receptor in the $Ca^{2+}$ wave trigger zone of pancreatic acinar cells. *J. Biol. Chem.* 269:4693–4696.

Newton, C.L., G.A. Mignery, and T.C. Südhof. 1994. Co-expression in vertebrate tissues and cell lines of multiple inositol 1,4,5-trisphosphate ($InsP_3$) receptors with distinct affinities for $InsP_3$. *J. Biol. Chem.* 269:28613–28619.

Nucifora, F.C., Jr., A.H. Sharp, S.L. Milgram, and C.A. Ross. 1996. Inositol 1,4,5-trisphosphate receptors in endocrine cells: localization and association in hetero- and homotetramers. *Mol. Biol. Cell.* 7:949–960.

Parekh, A.B., A. Fleig, and R. Penner. 1997. The store-operated calcium current $I_{CRAC}$: nonlinear activation by $InsP_3$ and dissociation from calcium release. *Cell.* 89:973–980.

Parys, J., S. Sernett, S. DeLisle, P. Snyder, M. Welsh, and K. Campbell. 1992. Isolation, characterization, and localization of the inositol 1,4,5-trisphosphate receptor protein in *Xenopus laevis* oocytes. *J. Biol. Chem.* 267:18776–18782.

Perez, P.J., J. Ramos-Franco, M. Fill, and G.A. Mignery. 1997. Identification and functional reconstitution of the type 2 inositol 1,4,5-trisphosphate receptor from ventricular cardiac myocytes. *J. Biol. Chem.* 272:23961–23969.

Putney, J.W., Jr., and G.S. Bird. 1993. The inositol phosphate-cal-

cium signaling system in nonexcitable cells. *Endocr. Rev.* 14:610–631.

Putney, J.W., Jr. 1997. Type 3 inositol 1,4,5-trisphosphate receptor and capacitative calcium entry. *Cell Calc.* 21:257–261.

Ramos-Franco, J., S. Caenepeel, M. Fill, and G. Mignery. 1998a. Single channel function of recombinant type-1 inositol 1,4,5-trisphosphate receptor ligand binding domain splice variants. *Biophys. J.* 75:2783–2793.

Ramos-Franco, J., M. Fill, and G.A. Mignery. 1998b. Isoform-specific function of single inositol 1,4,5-trisphosphate receptor channels. *Biophys. J.* 75:834–839.

Ramos-Franco, J., D. Galvan, G.A. Mignery, and M. Fill. 1999. Location of the permeation pathway in the recombinant type I inositol 1,4,5-trisphosphate receptor. *J. Gen. Physiol.* 114:243–250.

Rooney, T.A., and A.P. Thomas. 1993. Intracellular calcium waves generated by Ins(1,4,5)$P_3$-dependent mechanisms. *Cell Calc.* 14: 674–690.

Soreq, H., and S. Seidman. 1992. *Xenopus* oocyte microinjection: from gene to protein. *Methods Enzymol.* 207:225–265.

Stehno-Bittel, L., A. Lückhoff, and D.E. Clapham. 1995. Calcium release from the nucleus by Ins$P_3$ receptor channels. *Neuron.* 14: 163–167.

Stühmer, W. 1992. Electrophysiological recording from *Xenopus* oocytes. *Methods Enzymol.* 207:319–338.

Sudhof, T.C., C.L. Newton, B.T.I. Archer, Y.A. Ushkaryov, and G.A. Mignery. 1991. Structure of a novel Ins$P_3$-receptor. *EMBO (Eur. Mol. Biol. Organ.) J.* 10:3199–3206.

Sugiyama, T., A. Furuya, T. Monkawa, M. Yamamoto-Hino, S. Satoh, K. Ohmori, A. Miyawaki, N. Hanai, K. Mikoshiba, and M. Hasegawa. 1994. Monoclonal antibodies distinctively recognizing the subtypes of inositol 1,4,5-trisphosphate receptor: application to the studies on inflammatory cells. *FEBS Lett.* 354:149–154.

Supattapone, S., P.F. Worley, J.M. Baraban, and S.H. Snyder. 1988. Solubilization, purification and isolation of an inositol trisphosphate receptor. *J. Biol. Chem.* 263:1530–1534.

Taylor, C.W., and A. Richardson. 1991. Structure and function of inositol trisphosphate receptors. *Pharmacol. Ther.* 51:97–137.

Toescu, E.C. 1995. Temporal and spatial heterogeneities of $Ca^{2+}$ signaling: mechanisms and physiological roles. *Am. J. Physiol.* 269: G173–G185.

Watras, J., I. Bezprozvanny, and B.E. Ehrlich. 1991. Inositol 1,4,5-trisphosphate-gated channels in cerebellum: presence of multiple conductance states. *J. Neurosci.* 11:3239–3245.

Wojcikiewicz, R.J.H., T. Furuichi, S. Nakade, K. Mikoshiba, and S.R. Nahorski. 1994. Muscarinic receptor activation down-regulates the type I inositol 1,4,5-trisphosphate receptor by accelerating its degradation. *J. Biol. Chem.* 269:7963–7969.

Wojcikiewicz, R.J.H. 1995. Type I, II, and III inositol 1,4,5-trisphosphate receptors are unequally susceptible to down-regulation and are expressed in markedly different proportions in different cell types. *J. Biol. Chem.* 270:11678–11683.

Wojcikiewicz, R.J.H., and Y. He. 1995. Type I, II and III inositol 1,4,5-trisphosphate receptor coimmunoprecipitation as evidence for the existence of heterotetrameric receptor complexes. *Biochem. Biophys. Res. Commun.* 213:334–341.

Yamada, N., Y. Makino, R.A. Clark, D.W. Pearson, M.-G. Mattei, J.-L. Guénet, E. Ohama, I. Fujino, A. Miyawaki, T. Furuichi, and K. Mikoshiba. 1994. Human inositol 1,4,5-trisphosphate type-1 receptor, Ins$P_3$R1: structure, function, regulation of expression and chromosomal localization. *Biochem. J.* 302:781–790.

Yamamoto-Hino, M., T. Sugiyama, K. Hikichi, M.G. Mattei, K. Hasegawa, S. Sekine, K. Sakurada, A. Miyawaki, T. Furuichi, M. Hasegawa, and K. Mikoshiba. 1994. Cloning and characterization of human type 2 and type 3 inositol 1,4,5-trisphosphate receptors. *Receptors Channels.* 2:9–22.

Yao, Y., and R.Y. Tsien. 1997. Calcium current activated by depletion of calcium stores in *Xenopus* oocytes. *J. Gen. Physiol.* 109:703–715.

Yoshikawa, S., T. Tanimura, A. Miyawaki, M. Nakamura, M. Yuzaki, T. Furuichi, and K. Mikoshiba. 1992. Molecular cloning and characterization of the inositol 1,4,5-trisphosphate receptor in *Drosophila melanogaster. J. Biol. Chem.* 267:16613–16619.

Yule, D.I., S.A. Ernst, H. Ohnishi, and R.J.H. Wojcikiewicz. 1997. Evidence that zymogen granules are not a physiologically relevant calcium pool—defining the distribution of inositol 1,4,5-trisphosphate receptors in pancreatic acinar cells. *J. Biol. Chem.* 272: 9093–9098.